12-14-2015

Mist1 Expressing Gastric Stem Cells Maintain the Normal and Neoplastic Gastric Epithelium and Are Supported by a Perivascular Stem Cell Niche

Yoku Hayakawa
Vagelos College of Physicians and Surgeons

Hiroshi Ariyama
Vagelos College of Physicians and Surgeons

Jitka Stancikova
Institute of Molecular Genetics of the Academy of Sciences of the Czech Republic

Kosuke Sakitani
Vagelos College of Physicians and Surgeons

Samuel Asfaha
Vagelos College of Physicians and Surgeons

See next page for additional authors

Article

Cancer Cell

Mist1 Expressing Gastric Stem Cells Maintain the Normal and Neoplastic Gastric Epithelium and Are Supported by a Perivascular Stem Cell Niche

Graphical Abstract

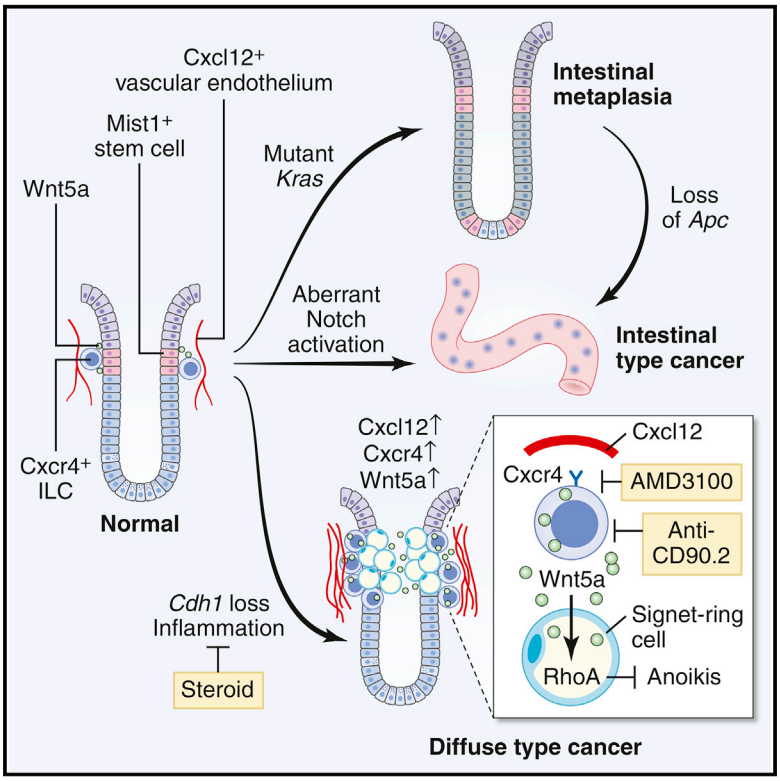

Highlights

- Quiescent Mist1$^+$ stem cells reside in the corpus isthmus
- Mist1$^+$ stem cells are a cellular origin of gastric cancers
- Cxcl12/Cxcr4 perivascular niche supports isthmus stem cells
- Wnt5a from Cxcr4$^+$ ILCs promotes diffuse cancer development

Authors

Yoku Hayakawa, Hiroshi Ariyama, Jitka Stancikova, ..., Daniel L. Worthley, Vladimir Korinek, Timothy C. Wang

Correspondence

tcw21@columbia.edu

In Brief

Hayakawa et al. show that Cxcl12$^+$ endothelial cells and Cxcr4$^+$ gastric innate lymphoid cells (ILCs) form a perivascular niche to support diffuse-type gastric cancer (DGC) development from Mist1-expressing gastric stem cells through Wnt5a produced by ILCs. Targeting ILCs, Cxcr4, or Wnt5a inhibits DGC development.

Hayakawa et al., 2015, Cancer Cell *28*, 800–814
December 14, 2015
http://dx.doi.org/10.1016/j.ccell.2015.10.003

CellPress

Cancer Cell
Article

Mist1 Expressing Gastric Stem Cells Maintain the Normal and Neoplastic Gastric Epithelium and Are Supported by a Perivascular Stem Cell Niche

Yoku Hayakawa,[1,12] Hiroshi Ariyama,[1,12] Jitka Stancikova,[2] Kosuke Sakitani,[1] Samuel Asfaha,[1] Bernhard W. Renz,[1,11] Zinaida A. Dubeykovskaya,[1] Wataru Shibata,[1] Hongshan Wang,[1] Christoph B. Westphalen,[1] Xiaowei Chen,[1] Yoshihiro Takemoto,[1] Woosook Kim,[1] Shradha S. Khurana,[1] Yagnesh Tailor,[1] Karan Nagar,[1] Hiroyuki Tomita,[3] Akira Hara,[3] Antonia R. Sepulveda,[4] Wanda Setlik,[5] Michael D. Gershon,[5] Subhrajit Saha,[6] Lei Ding,[7] Zeli Shen,[8] James G. Fox,[8] Richard A. Friedman,[9] Stephen F. Konieczny,[10] Daniel L. Worthley,[1] Vladimir Korinek,[2] and Timothy C. Wang[1,*]

[1]Division of Digestive and Liver Disease, Department of Medicine, Columbia University College of Physicians and Surgeons, New York, NY 10032, USA
[2]Department of Cell and Developmental Biology, Institute of Molecular Genetics, Academy of Sciences of the Czech Republic, Prague 14220, Czech Republic
[3]Department of Tumor Pathology, Gifu University Graduate School of Medicine, Gifu 501-1194, Japan
[4]Division of Clinical Pathology and Cell Biology, Department of Pathology, Columbia University College of Physicians and Surgeons, New York, NY 10032, USA
[5]Department of Pathology and Cell Biology, Columbia University College of Physicians and Surgeons, New York, NY 10032, USA
[6]Department of Radiation Oncology, Albert Einstein College of Medicine, Bronx, NY 10461, USA
[7]Departments of Rehabilitation and Regenerative Medicine and Microbiology and Immunology, Columbia University College of Physicians and Surgeons, New York, NY 10032, USA
[8]Division of Comparative Medicine, Massachusetts Institute of Technology, Cambridge, MA 02139, USA
[9]Herbert Irving Comprehensive Cancer Center Biomedical Informatics Shared Resource and Department of Biomedical Informatics, Columbia University College of Physicians and Surgeons, New York, NY 10032, USA
[10]Department of Biological Sciences and the Purdue Center for Cancer Research, Purdue University, West Lafayette, IN 47907, USA
[11]Department of General, Visceral, Transplantation, Vascular, and Thoracic Surgery, Hospital of the University of Munich, Munich 81377, Germany
[12]Co-first author
*Correspondence: tcw21@columbia.edu
http://dx.doi.org/10.1016/j.ccell.2015.10.003

SUMMARY

The regulation and stem cell origin of normal and neoplastic gastric glands are uncertain. Here, we show that Mist1 expression marks quiescent stem cells in the gastric corpus isthmus. Mist1$^+$ stem cells serve as a cell-of-origin for intestinal-type cancer with the combination of *Kras* and *Apc* mutation and for diffuse-type cancer with the loss of E-cadherin. Diffuse-type cancer development is dependent on inflammation mediated by Cxcl12$^+$ endothelial cells and Cxcr4$^+$ gastric innate lymphoid cells (ILCs). These cells form the perivascular gastric stem cell niche, and Wnt5a produced from ILCs activates RhoA to inhibit anoikis in the E-cadherin-depleted cells. Targeting Cxcr4, ILCs, or Wnt5a inhibits diffuse-type gastric carcinogenesis, providing targets within the neoplastic gastric stem cell niche.

INTRODUCTION

Gastric cancer is the third most frequent cause of cancer death worldwide. In the gastric corpus within the proximal stomach, the glands contain chief cells that are important for digestion, and parietal cells that are vital for acid production, controlled in part by enterochromaffin-like (ECL) cells. There are also intervening mucous neck cells, above which are the superficial pits that are lined by pit cell epithelium. Despite abundant literature on small intestinal stem cells (ISCs), an infrequent site of human

Significance

We identified a quiescent stem cell in the corpus isthmus, which can give rise to gastric cancer. We also discovered a Cxcl12/Cxcr4 perivascular niche in the stomach, which supports normal and neoplastic stem cells through Wnt5a production.

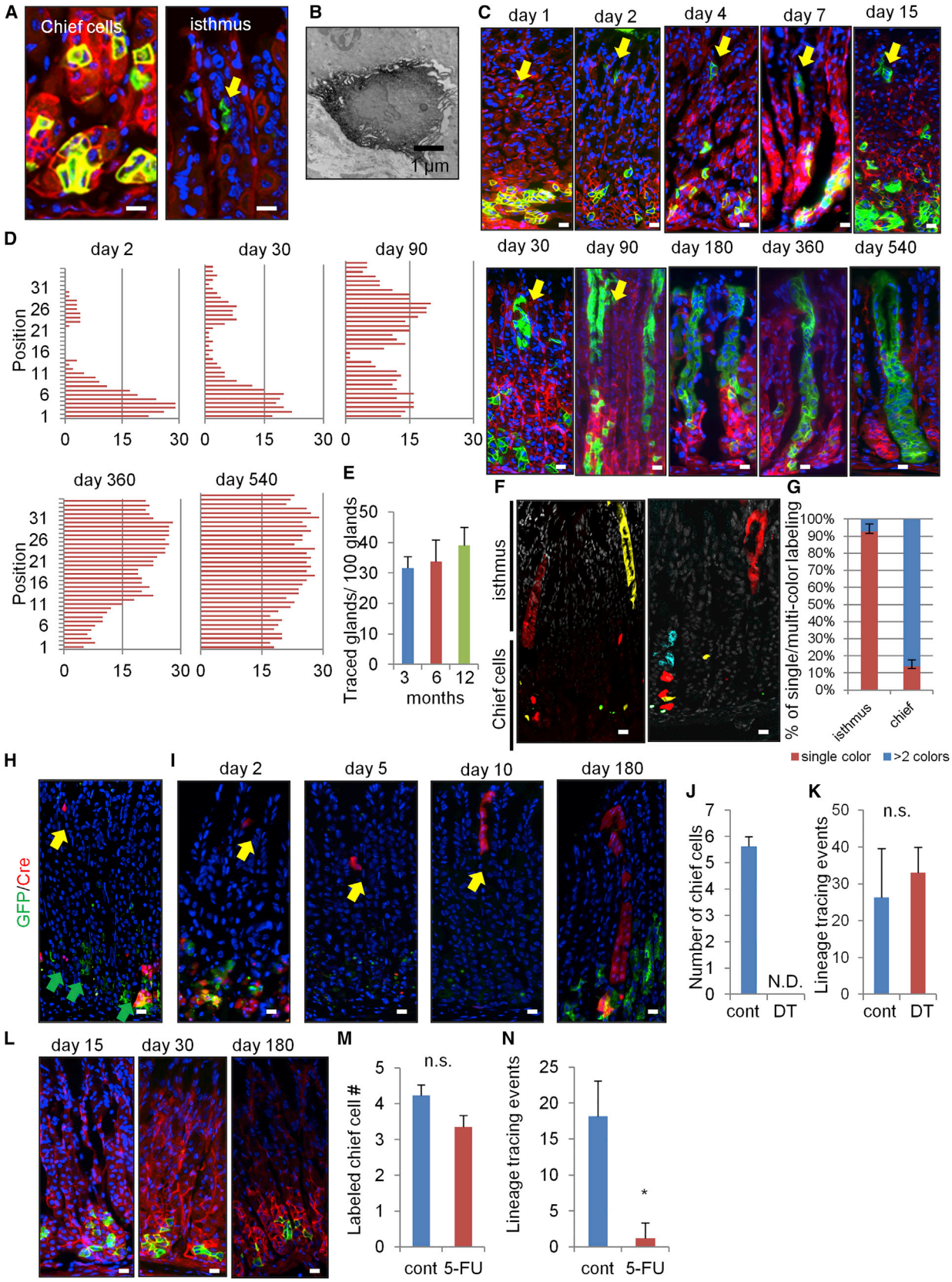

(legend on next page)

cancer, there have been relatively few studies addressing the stem cells that maintain the normal and neoplastic gastric epithelium.

Tissue stem cells maintain the integrity of rapidly proliferating tissues such as the gastrointestinal epithelium, residing within a stem cell niche. Replicative quiescence and a relatively undifferentiated morphology have generally been considered cardinal properties of adult stem cells (Malam and Cohn, 2014; Mills and Shivdasani, 2011). In the gastric corpus, earlier radiolabeling and electron microscopy studies suggest a single undifferentiated, ''granule free'' cell as the putative stem cell in the isthmus of each gastric unit of the mouse (Karam and Leblond, 1993; Mills and Shivdasani, 2011). Studies suggest that within the corpus isthmus, Sox2$^+$ cells may be long-lived stem cells, while Tff2$^+$ cells are relatively short-lived progenitors (Arnold et al., 2011; Quante et al., 2010). More recently, a ''reserve stem-like cell'' population expressing *Troy* or *Mist1* was postulated to reside at the base of corpus gland (Stange et al., 2013).

Gastric cancer is classified into an intestinal-type and a diffuse-type, and carcinogenesis in the stomach is strongly associated with chronic inflammation. Oncogenic mutations such as *Kras* and *Apc* targeted to gastric stem/progenitor cells led to intestinal-type metaplasia or dysplasia in mice (Barker et al., 2010; Okumura et al., 2010). By contrast, the E-cadherin gene (*CDH1)* is frequently mutated or downregulated in diffuse-type gastric cancer (DGC) (Guilford et al., 1998). In a rodent model, knock out of *Cdh1* was insufficient to initiate gastric tumors, but did predispose to the development of DGC with signet-ring cells following additional genetic events (Shimada et al., 2012). Studies of prophylactic gastrectomy specimens from germline carriers of *CDH1* mutations have revealed that DGC appears to arise in the proximal gastric isthmus (Humar et al., 2007), but the cellular origin of all gastric cancers remains unknown.

Tissue stem cells and cancer development are maintained by their niche. The Wnt signaling pathway plays a central role in the maintenance of ISCs, which are supported by the ISC niche, including both Paneth cells (Sato et al., 2011) and the surrounding mesenchyme (Farin et al., 2012). However, the gastric corpus does not normally depend on the Wnt pathway (Mills and Shivdasani, 2011), and therefore the critical pathway regulating corpus stem cell niche is largely unknown. In the gut mesenchyme, several cell types including pericytes, nerves, or mesothelial cells (Miyoshi et al., 2012; Worthley et al., 2015; Zhao et al., 2014) are reported to maintain tissue stem cells and contribute to cancer development. In the bone marrow, perivascular stromal cells including endothelial cells, Cxcl12-abundant reticular (CAR) cells, and nerves, promote hematopoietic stem cell (HSC) maintenance and neoplastic changes through the production of cytokines or chemokines such as Cxcl12 or SCF (Hanoun et al., 2014; Mendelson and Frenette, 2014; Pitt et al., 2015). However, whether such stromal factors play a role in the normal and neoplastic gut stem cell niche remains unclear.

RESULTS

Mist1 Is a Marker of Quiescent Stem Cells in the Gastric Corpus Isthmus

We utilized *Mist1*-CreERT2 knockin mice, where Cre recombinase is induced by tamoxifen (TAM) in cells expressing a bHLH transcription factor Mist1, and investigated the contribution of Mist1$^+$ reserve stem-like chief cells to gastric carcinogenesis. To clarify the expression pattern of *Mist1* in the normal stomach, we crossed *Mist1*-CreERT2 mice with *R26*-mTmG mice. This reporter features the dichotomous expression of red (without recombination) or green fluorescence (with recombination). Most of the recombined Mist1$^+$ cells were detected in mature chief cells in the lower third of the glands (position 1–14) 1 day after TAM induction (Figure 1A). However, Mist1$^+$ recombined cells were also evident as rare single cells in the isthmus. Recombination in the isthmus was observed in either *R26*-TdTomato or *R26*-LacZ mice, or with low dose TAM (1 mg) (Figure S1A). Endogenous *Mist1* expression in the isthmus was confirmed by in situ hybridization (Figure S1B). Their electron microscopy appearance was similar to the granule free stem cells previously reported (Karam and Leblond, 1993) (Figure 1B).

The GFP$^+$ Mist1 lineage expanded gradually over 540 days (Figures 1C and 1D). In contrast to a previous report (Stange et al., 2013), our detailed time course revealed bi-directional expansion from single Mist1$^+$ cells at position 25–30 in the isthmus, both upward toward the lumen and deeper into the gland, independent of the dose of TAM (Figure S1C). The approximate doubling time of Mist1$^+$ isthmus cells is 120 hr or 5 days (Figure S1D), and these cells first divided into isthmus progenitors with small or spindle appearance (Figure S1E),

Figure 1. Mist1 Is a Marker of Quiescent Stem Cells in the Corpus Isthmus

(A) The corpus of *Mist1*-CreERT2;*R26*-mTmG mice day 1 after 3 mg TAM. The left image shows chief cells and the right image shows isthmus cells (arrow).

(B) Electron microscopy of Mist1$^+$ cells in the isthmus.

(C) Lineage tracing in *Mist1*-CreERT2;*R26*-mTmG mice from day 1–540. The arrow indicates the isthmus cells.

(D) Mist1-traced cell position. The total 50 glands are analyzed at each time point.

(E) The number of traced glands per 100 glands at 3, 6, and 12 months. The total 300 glands from three mice are used at each time point.

(F and G) *Mist1*-CreERT2;*R26*-Confetti mice 8 months after TAM (F). The single color and multi-color clones in the isthmus and chief cells are quantified (G). The total 50 glands are analyzed.

(H and I) *Mist1*-CreERT2;*Lgr5*-DTR-GFP (green);*R26*-TdTomato (red) mouse corpus 24 hr after TAM (H) and 2, 5, 10, and 180 days after TAM + DT ablation (I). The yellow arrows show Mist1$^+$ isthmus cell tracing and the green arrows show Lgr5$^+$ chief cells.

(J and K) The numbers of labeled chief cells per gland (J, day 4) and lineage tracing events per 100 glands (K, day 30) with or without DT ablation.

(L) Lineage tracing in 5-FU-treated *Mist1*-CreERT2;*R26*-mTmG mouse corpus (refer to Figure 1C for control images).

(M and N) The numbers of labeled chief cells per gland 4 days after TAM (cont) or TAM + 5-FU (5-FU) treatments (M) and the number of lineage tracing events per 100 glands on day 30 (N). The total 500 glands from five mice/group are analyzed for (J), (K), (M), and (N). Scale bars represent 1 μm (B) and 10 μm (A, C, F, H, I, and L) (means ± SEM) (*$p < 0.05$).

See also Figure S1.

followed later by the differentiation into surface pit and neck cells and subsequently into parietal cells. Over time, the number of GFP$^+$ cells in the chief cell region declines while the isthmus clone expands (Figure 1D). Lineage tracing persisted beyond 18 months post-induction with whole labeled corpus glands, proving that Mist1$^+$ cells self-renew (Figure 1E). *Mist1*-CreERT2;*R26*-Confetti mice show that single-color clonal expansion is seen predominantly in the isthmus area, while chief cells show scattered multi-color labeling (Figures 1F and 1G). These data indicate that the Mist1$^+$ isthmus cell is the major source of lineage tracing of corpus glands.

In this period, Mist1$^+$ cells gave rise to mucus neck cells (GS-II), parietal cells (H/K-ATPase), surface pit cells (TFF1), tuft cells (Dclk1), and ECL cells (chromogranin A), while initially Mist1$^+$ cells were negative for these markers (Figures S1F and S1G). Mist1$^+$ chief cells at the base of glands are as expected positive for GIF at day 2 after TAM, while the Mist1$^+$ isthmus cells are GIF-negative (Figure S1H). However, the early traced GIF$^+$ chief cells at the base of glands decreased over time with an increase of traced GIF$^-$ isthmus cells (Figures S1I and S1J). Thus, Mist1$^+$ basal chief cells are labeled by initial TAM induction, but these cells turn over and disappear, finally to be renewed from the isthmus-derived Mist1$^+$ stem cell.

Mist1$^+$ Isthmus Cells Are Responsible for Gastric Lineage Tracing

We confirmed no overlap between Mist1$^+$ cells and reported gastric stem cell markers Cckbr$^+$ or Sox2$^+$ (Arnold et al., 2011; Hayakawa et al., 2015) (Figures S1K and S1L). Since chief cells have also been shown to be Lgr5$^+$ (Stange et al., 2013), we generated *Mist1*-CreERT2;*Lgr5*-DTR-GFP;*R26*-Tdtomato mice (Tian et al., 2011). Similar to GIF staining, the vast majority of Mist1$^+$ chief cells at the base are Lgr5$^+$, whereas the Mist1$^+$ isthmus cells are Lgr5$^-$ (Figure 1H). Thus, we ablated Lgr5$^+$ cells, which included Mist1$^+$ chief cells, by administration of diphtheria toxin (DT) (Figure S1M). After giving TAM and DT, 100% of labeled chief cells were ablated (Figures 1I, 1J, and S1N). The expression of *Lgr5* or *Gif* was markedly reduced by DT ablation (Figure S1O). However, the number of isthmus Mist1$^+$ cells was even increased and lineage tracing occurred at the same frequency as the control (non-DT) group, accompanied with faster cell division (Figures 1I, 1K, and S1P–S1S). After 6 months, the isthmus Mist1$^+$ cells gave rise to chief cells. Similarly, ablation of chief cells by the elastase inhibitor DMP-777 (Nomura et al., 2005) did not affect the frequency of lineage tracing (Figures S1T–S1W). In contrast, when we treated mice with 5-Fluorouracil (5-FU) to kill isthmus stem/progenitor cells (Figures S1X and S1Y) (Stange et al., 2013), the mice showed almost no lineage tracing events, but maintained a similar number of labeled chief cells at the gland base for 6 months (Figures 1L–1N). Thus, Mist1$^+$ isthmus cells, and not Mist1$^+$ chief cells, are responsible for lineage tracing in the corpus.

Isthmus Mist1$^+$ Cells Give Rise to Intestinal-type Metaplasia and Cancer

In the isthmus, 1.1% of the Mist1$^+$ cells were Ki67$^+$ (Figure 2A), thus, more than 98% of Mist1$^+$ isthmus stem cells are quiescent. *KRAS* is one of the most commonly mutated proto-oncogenes in a variety of cancers, including gastric cancer. To investigate the effect of *Kras* mutation in gastric stem cells, we crossed *Mist1*-CreERT2 mice to LSL-*Kras*^{G12D} mutant mice. *Kras* mutation in Mist1$^+$ isthmus cells resulted in an increased percentage of Ki67$^+$Mist1$^+$ cells and overall faster cell division (Figures S2A–S2C). These cells formed Ki67$^+$ dysplastic foci in the isthmus, which contained Alcian blue positive metaplastic cells (Figures 2B–2D). The metaplastic/dysplastic foci moved from the isthmus to the bottom of glands with loss of parietal cells and chief cells and eventually replaced the entire glands with intestinal metaplasia (IM) and dysplasia (Figure S2D). We generated *Mist1*-CreERT2;LSL-*Kras*^{G12D};*Lgr5*-DTR mice and ablated isthmus cells and chief cells by giving 5-FU and DT, accordingly, after TAM induction (Figure S2E). Strikingly, 5-FU inhibited the metaplasia development, while DT ablation did not (Figures 2E and 2F), indicating that the Mist1$^+$ isthmus cells, and not the Mist1$^+$ chief cells, are an origin of *Kras*-induced IM and dysplasia.

Aberrant activation of the Wnt signaling pathway by inactivating *Apc* is a common initiating event in many gastrointestinal tumors (Barker et al., 2009, 2010). Thus, we established *Mist1*-CreERT2;*Apc*$^{flox/flox}$ mice. Nuclear accumulation of β-catenin was observed in the Mist1$^+$ lineage (isthmus and chief cells). However, nuclear β-catenin$^+$ cells in corpus Mist1$^+$ cells did not form dysplasia at later time points (up to 8 months) (Figures 2G and 2H), which seems contrary to the phenotype of *Apc* loss in stem cells in the gastric antrum, small intestine, and colon. In fact, whereas Wnt inhibition by Dickkopf-1 (DKK1) overexpression leads to marked decrease in proliferation in the intestine and colon, proliferation in the corpus was not inhibited (Figures S2F and S2G), suggesting that tumor initiation or proliferation in the corpus is likely independent of Wnt/β-catenin signaling.

IM in the stomach is a known risk factor or precursor lesion for intestinal-type gastric cancer (IGC). Thus, we attempted to induce Wnt/β-catenin activation in the presence of IM. We generated *Mist1*-CreERT2;LSL-*Kras*^{G12D};*Apc*$^{flox/flox}$ mice, and this mouse developed intramucosal IGC with the expansion of nuclear β-catenin$^+$ cells in 4 months (Figure 2I). Thus, Mist1$^+$ stem cells can give rise to IGC with loss of *Apc* only when *Kras*-induced IM is also present. Notch signaling is another important pathway regulating gastric proliferation (Kim and Shivdasani, 2011). The Notch inhibitor dibenzazepine (DBZ) reduced the expansion of *Mist1*-lineage tracing as well as proliferation in the isthmus (Figures S2H–S2K), and constitutive activation of Notch signaling in Mist1$^+$ stem cells by generating Mist1-CreERT2;*Eef1a1*-LSL-*Notch1(IC)* mice (Buonamici et al., 2009) resulted in the development of IGC (Figure S2L). Although Mist1 protein expression is decreased in *Kras*/*Apc*-induced IGC, aberrant Notch activation increased the number of Mist1$^+$ cells in the tumor (Figures S1Q and S2M). The dysplastic cells in Notch-induced tumor did not display nuclear β-catenin accumulation, suggesting that in the corpus, Notch signaling is a Wnt-independent oncogenic pathway through which Mist1$^+$ stem cells can progress to IGC.

Mist1$^+$ Isthmus Cells Can Form Corpus Organoids in a Lgr5-Independent Fashion

To evaluate the stem cell properties of Mist1$^+$ cells in vitro, we isolated corpus glands from *Mist1*-CreERT2;*R26*-mTmG mice 1 day following TAM induction. Mist1$^+$ green cells were observed

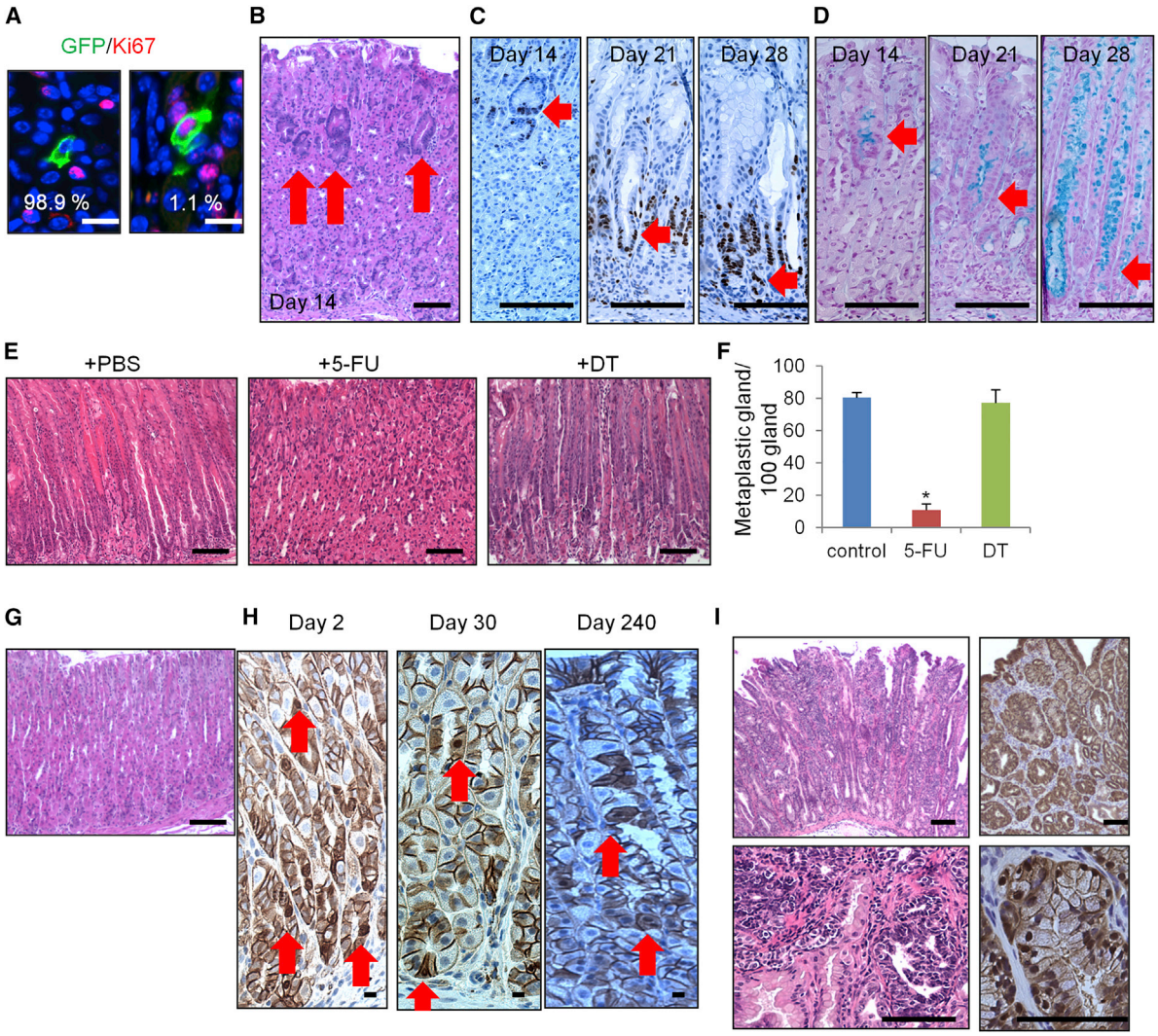

Figure 2. Mist1^{+} Isthmus Cells Give Rise to IM and IGC

(A) Ki67 (red) and GFP staining (green) of *Mist1*-CreERT2;*R26*-mTmG mice at day 2.

(B–D) Hematoxylin and eosin (H&E) (B), Ki67 (C), and Alcian blue (D) staining in *Mist1*-CreERT2;LSL-*Kras*^{G12D} mice on days 14, 21, and 28 after induction. The arrows indicate isthmus-derived dysplastic cells.

(E and F) H&E staining (E) and numbers of metaplastic glands per 100 glands (F) of *Mist1*-CreERT2;LSL-*Kras*^{G12D};*Lgr5*-DTR-GFP mice treated with PBS (left), 5-FU (middle), or DT (right) 30 days after TAM. The total 300 glands from three mice/group are analyzed.

(G and H) H&E (G, day 240) and β-catenin (H) staining in *Mist1*-CreERT2;*Apc*$^{flox/flox}$ mouse. The arrows indicate the nuclear β-catenin^{+} cells.

(I) H&E (left) and β-catenin (right) staining in *Mist1*-CreERT2;LSL-*Kras*^{G12D};*Apc*$^{flox/flox}$ mouse corpus on day 120 post-induction (means ± SEM) (*$p < 0.05$). Scale bars represent 10 μm (A) and 100 μm (B–E and G–I).

See also Figure S2.

in the two distinct positions, and Mist1^{+} isthmus cells expanded to form cystic organoids in the reported culture method (Stange et al., 2013), while Mist1^{+} chief cells remained as single cells and eventually disappeared (Figure 3A). The GFP^{+} Mist1-derived cells survived in vitro for at least 2 months, confirming longevity. Even after ablation of Lgr5^{+} chief cells in *Mist1*-CreERT2;*Lgr5*-DTR;*R26*-TdTomato mice by DT injection, isthmus Mist1^{+} cells continued to lineage trace and give rise to chief cells in cultured organoids (Figures 3B and 3C). We next sorted Mist1^{+} cells after DT or 5-FU treatment to the mice (lacking chief cells and isthmus cells, respectively) (Figures 3D–3F). Colony formation efficiency increased in the DT-treated group and decreased in the 5-FU-treated group, suggesting that isthmus Mist1^{+} cells are the true corpus stem cells, rather than Mist1^{+} chief cells. We compared gene expression patterns between the total Mist1^{+} population (majority of which were chief cells), DT-ablated isthmus Mist1^{+} population, and the differentiated parietal cell population (Figure S3A). *Lgr5* and *Gif* expression are markedly downregulated in isthmus Mist1^{+} cells compared to total Mist1^{+} cells. *Mist1* expression is upregulated in both total and isthmus Mist1^{+} population. The expression of several stem/progenitor markers, such as *Cd44* and *Sox9*, or target genes of Wnt and Notch

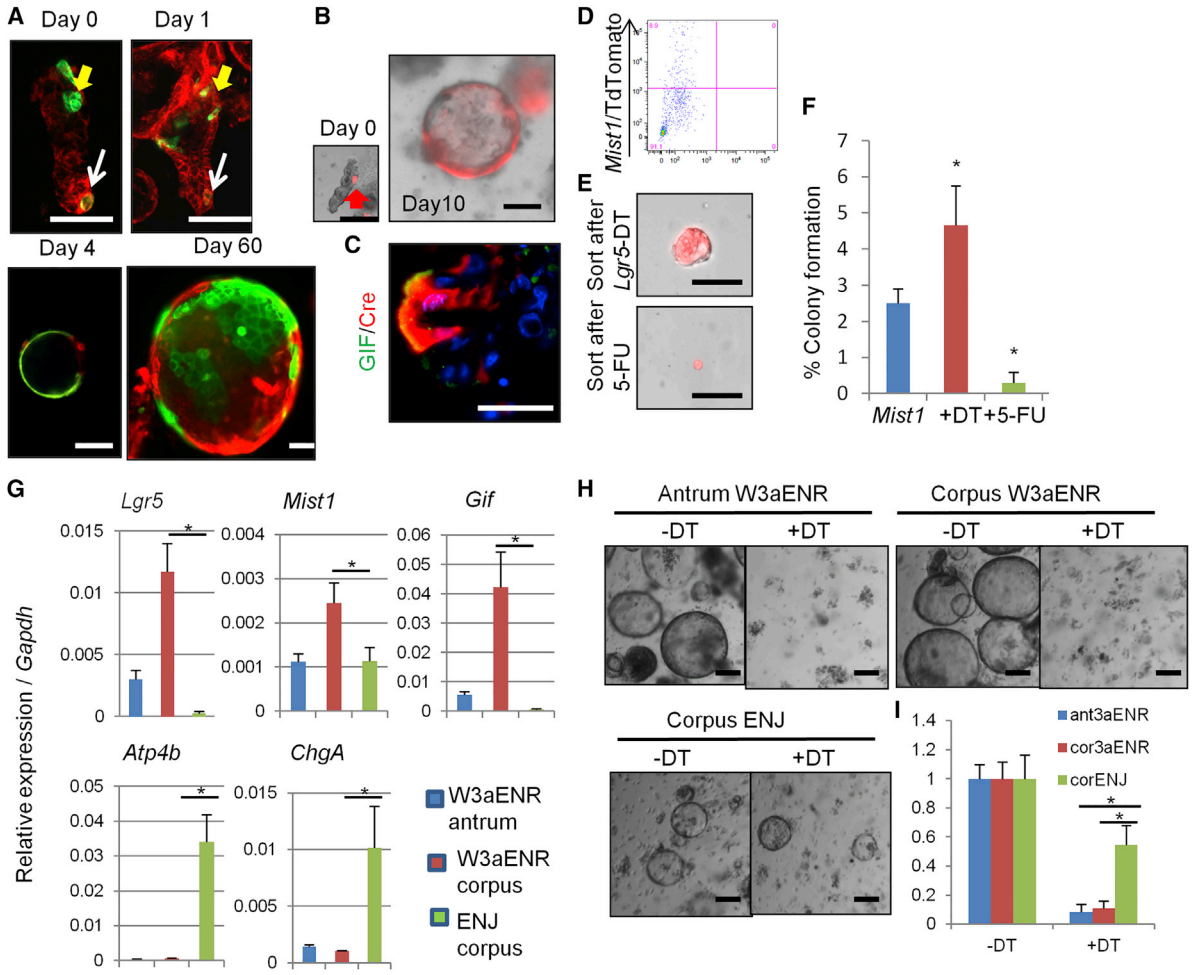

Figure 3. Mist1$^+$ Isthmus Cells Can Form Corpus Organoids in a Lgr5-Independent Fashion

(A) Corpus gland culture of TAM-induced *Mist1*-CreERT2;*R26*-mTmG mice. The yellow arrows show isthmus cells and the white arrows show chief cells.

(B and C) Lineage tracing (B) and GIF staining (C, green) of corpus gland culture from *Mist1*-CreERT2;*Lgr5*-DTR-GFP;*R26*-TdTomato mice treated with DT.

(D–F) TdTomato$^+$ cells were sorted and cultured from DT or 5-FU-treated *Mist1*-CreERT2;*Lgr5*-DTR-GFP;*R26*-TdTomato mice corpus after TAM. The FACS plot (D), images (E), and the colony formation efficiency (F) at day 7 are shown (n = 4/group).

(G) Relative gene expression per *Gapdh* in antral or corpus organoids cultured with the indicated media for 10 days (n = 3/group).

(H and I) Organoid growth of antrum and corpus glands cultured with W3aENR or ENJ media. The day 10 images (H) and the relative numbers of organoids cultured in the indicated media (I) are shown. The numbers in non-DT organoids in each group are set as 1.0 (n = 3/group) (means ± SEM) (*$p < 0.05$). Scale bars represent 50 μm.

See also Figure S3.

signaling, such as *Ccnd1*, *Notch1*, and *Hes1*, remain at higher levels in the isthmus population, suggesting that isthmus Mist1$^+$ cells are Lgr5$^-$, but still exhibit stem cell characteristics.

The Wnt3a/R-spondin1 (W3a/Rspo1)-dependent culture system fails to produce corpus-specific cell lineage such as parietal cells and ECL cells (Stange et al., 2013). Instead, W3aENR media (W3a, EGF, Noggin, and Rspo1) induces marked upregulation of *Lgr5* (three times higher than gastric antrum organoids) (Figure 3G). Compared to standard W3aENR media, culture of corpus glands in ENJ media (where Wnt3a/Rspo1 were replaced by Notch ligand Jagged-1) led to decreased expression of *Lgr5* or *Gif*, suggesting that Wnt3a/Rspo1 lead to expansion of chief cells. In contrast, in ENJ media, we observed greater amounts of parietal cells and ECL cells than in W3aENR media both in RT-PCR and immunostaining assays (Figures 3G and S3B), suggesting that the activation of Notch signaling is more important for preserving mature corpus cell types in culture than canonical Wnt signaling. Addition of a γ-secretase inhibitor blocked corpus organoid growth (Figures S3C and S3D), thus Notch signaling is important for corpus stem cell maintenance and growth. When we cultured *Mist1*-CreERT2;*Lgr5*-DTR;*R26*-TdTomato glands, antral and corpus organoids cultured with W3aENR did not grow and died following DT treatment (Figures 3H and 3I), indicating that organoid growth is highly dependent on Lgr5$^+$ cells in W3aENR media. However, lineage-traced corpus organoids survived with ENJ plus DT media (Figure S3E), proving that a non-Lgr5 stem cell population maintains organoid growth in Wnt3a/Rspo1-independent culture conditions.

Cxcl12^{+} Endothelium and Cxcr4^{+} ILCs Contribute to the Corpus Stem Cell Niche through Wnt5a Production

Given our in vitro data suggesting that Wnt3a or canonical Wnt signaling is not a critical niche factor in the corpus, we explored which Wnt ligands are indeed expressed in the stomach and intestine (Figures 4A and S4A). Among known Wnt ligands, *Wnt3a* expression was quite low in the corpus, in contrast to the intestine. Instead, an atypical Wnt ligand, *Wnt5a*, was highly expressed in the corpus. In situ hybridization of *Wnt5a* revealed focal expression in the isthmus stroma (Figure 4B) coincident with the known expression of Cxcr4 (Shibata et al., 2013). In *Cxcr4*-EGFP mice, Cxcr4^{+} cells were found in the isthmus area as rare single cells, showing almost identical distribution to *Wnt5a* expression (Figure 4C). Cxcr4^{+} cells and Mist1^{+} cells represent distinct populations, although they were located in close proximity within the isthmus (Figure 4D).

Immunostaining revealed that Cxcr4^{+} cells in the corpus are negative for E-cadherin or stromal markers, αSMA, NG2, and S100B, but positive for CD45, suggesting that they are tissue-resident hematopoietic cells recruited to the isthmus (Figures 4E and S4B). About 60% of gastric CD45^{+}Cxcr4^{+} cells from the whole gastric corpus are CD11b^{+} myeloid lineages (Figure S4C). CD3^{+} T cells, CD19^{+} B cells, and NK1.1^{+} classical NK cells are Cxcr4^{-}. The remaining 40% of CD45^{+}Cxcr4^{+} cells are Lineage-negative (CD3^{-}Gr1^{-}CD11b^{-}CD45R^{-}Ter119^{-}) and about half of the Lin^{-}Cxcr4^{+} population is a CD90.2^{+}CD127^{+} lymphoid population (Figures 4F and S4C). The other half is predominantly c-kit^{+}FcεRIα^{+} mast cells. Immunostaining defined the isthmus Cxcr4^{+} cells as Lin^{-}CD90.2^{+} intraepithelial gastric innate lymphoid cells (ILCs) (Figures 4E and S4D). *Id2*-GFP mice, which mark all types of ILCs (Hoyler et al., 2012), show a similar distribution pattern as Cxcr4^{+} cells (Figure S4E). The majority (90%) of gastric Cxcr4^{+} ILCs are NKp46^{-}CD4^{-}, Scal^{+}ICOS^{+}KLRG^{+} ILC2 cells, and a small population (5%) are Rorgt^{+}NKp46^{-} ILC3 cells (Figures 4F and S4F). In fact, the gastric Cxcr4^{+} ILC population is enriched with ILC2-specific genes (Figure S4G).

In the sorted Mist1^{+} cells and Cxcr4^{+} cells, *Wnt5a* was expressed primarily in the Cxcr4^{+} cells (Figures S4H and S4I), confirming our in situ hybridization findings. When we treated Cxcr4^{+} cells with Cxcl12 in vitro, *Wnt5a* expression was upregulated (Figure S4J). We hypothesized that the Cxcr4^{+} cell might be a niche cell, supporting gastric stem cell function. To test this possibility, we performed a co-culture experiment with "red" Mist1^{+} cells and "green" Cxcr4^{+} cells. Co-culture of Mist1^{+} cells with Cxcr4^{+} cells significantly enhanced red colony formation ability (Figures 4G and 4H). Treatment with Cxcl12 demonstrated an additive effect on Cxcr4^{+} cell co-culture, while it had no effect on Mist1^{+} cell culture alone, indicating that Cxcl12 acts through the Cxcr4^{+} ILCs. Furthermore, the Cxcr4^{+} ILC population exhibits the highest expression of *Wnt5a* compared to CD45^{+}Cxcr4^{-} cells or Cxcr4^{+} non-ILCs (Figure 4I). The colony formation ability of Mist1^{+} stem cells is enhanced by Wnt5a or co-culture with Cxcr4^{+} ILC population. However, *Wnt5a*-deficient ILCs which are sorted from *Cag*-CreERT2;*Wnt5a*$^{flox/flox}$ mouse stomach after TAM induction failed to show the same effect (Figure 4J). Thus, Cxcr4^{+}ILC-derived Wnt5a plays a key role for promoting Mist1^{+} stem cell colony formation.

We explored the source of Cxcl12 in the stomach. In *Cxcl12*-dsRED mice (Ding and Morrison, 2013), there were frequent dsRED^{+} cells in the stroma near the isthmus (Figure 4K). Indeed, Cxcr4^{+} ILCs and Cxcl12^{+} stromal cells in *Cxcr4*-EGFP;*Cxcl12*-dsRED mice were frequently positioned in close proximity (Figures 4L and 4M). We confirmed that Cxcl12^{+} cells are CD31^{+} and endomucin^{+} endothelial cells (Figures 4N and S4K). We compared RNA expression between dsRED^{+}CD31^{+} cells (35% of total CD31^{+} cells) and dsRED^{-}CD31^{+} cells by quantitative RT-PCR array (Figure S4L; Table S1). Among pathways potentially involved in the regulation of *Cxcl12* expression, we found that Cxcl12^{+} cells express BMP receptor 2, and BMP2 treatment in vitro upregulates *Cxcl12* expression (Figures S4M and S4N), consistent with previous findings (Yang et al., 2008). Interestingly, *Tie2*-Cre;*Cxcl12*$^{flox/flox}$;*Cxcr4*-EGFP mice, with targeted knock out of *Cxcl12* in endothelial cells, displayed a significant reduction in the number of Cxcr4^{+} cells in the isthmus compared to control mice (Figures 4O and 4P). Together, endothelial Cxcl12 is important for the recruitment of Wnt5a-producing Cxcr4^{+} ILCs in the stomach.

E-cadherin Loss in Mist1^{+} Cells Develops a Diffuse-type Cancer Dependent on Chronic Inflammation

We sought to establish whether Mist1^{+} stem cells were also a cell of origin for the DGC by knocking out the *Cdh1* gene in Mist1^{+} cells. *Mist1*-CreERT2;*Cdh1*$^{flox/flox}$ mice (*Cdh1*$^{\Delta Mist1}$) developed the pathognomonic, small mucous-producing atypical cell foci in the isthmus 10 days after TAM, but not in the chief cell region (Figures 5A and 5B). E-cadherin was downregulated in these atypical cells in the isthmus, consistent with early signet-ring cell morphology, recapitulating the earliest events in the pathogenesis of human signet-ring cell carcinoma. Ablation of chief cells and isthmus cells by DT and 5-FU treatment with *Mist1*-CreERT2;*Cdh1*$^{flox/flox}$;*Lgr5*-DTR mice confirmed that the isthmus Mist1^{+} cells are an origin of signet-ring cells (Figures S5A and S5B). Cxcl12/Cxcr4 niche cells were not affected by 5-FU treatment (data not shown).

Nevertheless, the number of atypical cells gradually declined and disappeared (Figure 5C), suggesting that E-cadherin loss leads to epithelial cell death and is on its own insufficient to initiate DGC. Given that mild inflammation without gastric atrophy is a common feature of DGC (Carneiro et al., 2004), we infected TAM-induced *Cdh1*$^{\Delta Mist1}$ mice with *Helicobacter felis* (*Hf*) to induce chronic inflammation. Surprisingly, in mice with *Hf* infection, atypical foci were preserved and expanded even after 1 year following TAM induction (Figure 5C). Lineage-traced DGC with numerous signet-ring cells was detected at 18 months post *Hf* infection in *Cdh1*$^{\Delta Mist1}$ mice (Figure 5D; seven of nine mice, 78%), along with the increase of Mist1^{+} cells in DGC (Figures S1Q and S5C). The addition of *Trp53* mutation in this setting led to invasive DGC within 9 months (Figure S5D). Interestingly, administration of dexamethasone to *Hf*-infected *Cdh1*$^{\Delta Mist1}$ mice reduced the number of signet-ring cell foci to the same level as non-infected control mice (Figures 5E–5G). In contrast, another inflammation-associated cancer model, H/K-ATPase-IL-1β transgenic mice (Tu et al., 2008), also showed a dramatic expansion of lineage-traced signet-ring cells when crossed to *Cdh1*$^{\Delta Mist1}$ mice, even without *Hf* infection (Figures 5H–5J). Thus, DGC development from Mist1^{+} stem cells is dependent

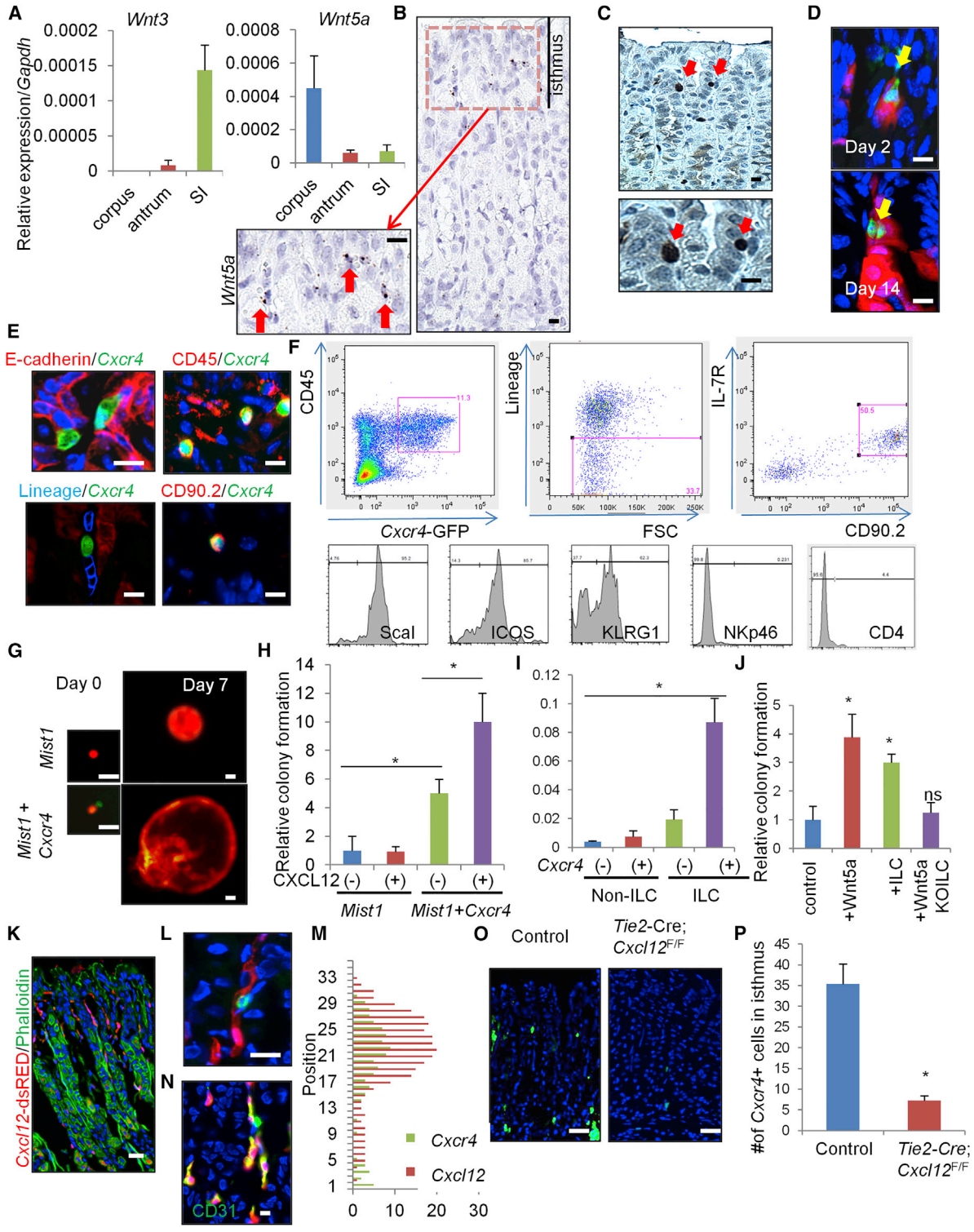

Figure 4. Cxcl12$^+$ Vascular Endothelial and Cxcr4$^+$ ILCs Contribute to Corpus Stem Cell Niche through Wnt5a Production

(A) Relative expression of *Wnt3* and *Wnt5a* in the corpus, antrum, and small intestine (n = 3/group).

(B) In situ hybridization of *Wnt5a* in the corpus. The arrows indicate the *Wnt5a*-expressing cells in the isthmus stroma.

(C) GFP staining in the *Cxcr4*-EGFP mouse corpus gland. The arrows indicate the GFP$^+$ cells in the isthmus.

(D) Lineage tracing in *Mist1*-CreERT2;*Cxcr4*-EGFP;*R26*-TdTomato mice on days 2 and 14. The arrows indicate the GFP$^+$ cells.

(E) E-cadherin (red), CD45 (red), Lineage (blue), and CD90.2 (red) staining of *Cxcr4*-EGFP$^+$ cells.

(legend continued on next page)

on chronic inflammation and anti-inflammatory therapy may be useful for preventing DGC.

Although Troy$^+$ chief cells are reported to act as reserve stem cells (Stange et al., 2013), we observed a rare Troy$^+$ population in the isthmus that could lineage trace and give rise to cancers by examining *Troy*-BAC-CreERT2 mice (Fafilek et al., 2013) (Figures S6A–S6G). Also, while Troy$^+$ chief cells with intact Troy expression do not proliferate and do not lineage trace, loss of *Troy* expression significantly promoted chief cell proliferation and lineage tracing after injury (Figures S6H–S6L), similar in most respects to the previous report, reconciling our findings with those of earlier groups (Stange et al., 2013).

Cxcl12/Cxcr4 Perivascular Niche Regulates DGC Progression through Wnt5a Production

During DGC development under chronic inflammation, corpus stem cell niche factors—Cxcl12$^+$ endothelium and Cxcr4$^+$ ILCs—are markedly expanded or upregulated in the region surrounding the isthmus DGC lesion (Figures 6A–6E), suggesting that these niche factors contribute to DGC development. We tested therapeutic intervention with AMD3100, a specific inhibitor of CXCR4, and an anti-CD90.2 antibody (Ab) for specific depletion of ILCs. Compared with vehicle-injected control mice, AMD3100 and the anti-CD90.2 Ab significantly reduced the number of signet-ring cell foci (Figures 6F–6H). In contrast, overexpression of *Cxcl12* in *Mist1*-CreERT2;H/K-ATPase-*Cxcl12*;*Cdh1*$^{flox/flox}$ mice led to persistence and growth of DGC lesions over 3 months even without *Hf* infection (Figures 6I–6K). *Hf* infection further accelerated DGC progression in this mouse model, while anti-CD90.2 Ab treatment significantly reduced the number of DGC foci in the setting of Cxcl12 overexpression (Figures S6M and S6N). Thus, upregulation of Cxcl12/Cxcr4 signaling through activation of ILCs plays a central role in DGC development.

After *Hf* infection, *Wnt5a* is highly upregulated in the stroma surrounding signet-ring lesions in the isthmus (Figure 6L). In addition, AMD3100 and anti-CD90.2 Ab treatment, or knock out of *Cxcl12* in Tie2-lineage, significantly decreased the number of Cxcr4$^+$ cells in the isthmus and the expression of *Wnt5a*, while Cxcl12-overexpression led to an increase in Cxcr4$^+$ cell number and upregulation of *Wnt5a* (Figures 6M and S6O). Thus, we tested the contribution of Wnt5a in DGC development by transplanting *Cag*-CreERT; *Wnt5a*$^{flox/flox}$ mouse bone marrow cells into *Cdh1*$^{\Delta Mist1}$ mice (Figure 6N). In these chimeric mice, E-cadherin is depleted in the Mist1$^+$ lineage and *Wnt5a* is knocked out in bone-marrow derived ILCs after TAM induction. *Cdh1*$^{\Delta Mist1}$ mice with *Cag*-CreERT;*Wnt5a*$^{flox/flox}$ bone marrow exhibited significantly fewer signet-ring cell foci compared to *Cdh1*$^{\Delta Mist1}$ mice with wild-type (WT) bone marrow cells (Figures 6O and 6P), indicating that Wnt5a in the hematopoietic cells promotes DGC progression. Although there was a significant increase in the number of Cxcr4$^+$ cells in the *Kras*-induced IGC model, AMD3100 failed to block either *Kras* or *Notch*-dependent IGC progression (Figures S6P and S6Q), suggesting the more predominant role of this pathway in DGC development.

RhoA Activation by Wnt5a Plays a Role in DGC Development

Wnt5a is known to activate a small GTPase protein, RhoA, which has a prosurvival effect by inhibiting anoikis in gastric and other cancer cells (Cai et al., 2008; Liu et al., 2013). Thus, we hypothesized that ILC-derived Wnt5a activates RhoA in E-cadherin-depleted cells and prolongs cell survival. We confirmed that Wnt5a activates RhoA in a *CDH1* mutant AGS cells by immunoprecipitation (Figure 7A). In a soft-agar assay, treatment of AGS cells with Wnt5a enhanced sphere formation, indicating that Wnt5a promotes anchorage-independent cell growth. Interestingly, blocking RhoA activation using a Rho inhibitor, Rhosin, diminished Wnt5a-mediated effects (Figures 7B and 7C). Similar results were observed with another DGC cell line, KATO-III. Furthermore, we found that E-cadherin-deficient Mist1$^+$ stem cells, which are normally unable to survive in vitro upon *Cdh1* deletion, displayed prolonged survival in the presence of Wnt5a (Figures 7D and 7E). This prosurvival effect was blocked by Rhosin, suggesting that Wnt5a-mediated RhoA activation is a key event for the survival of *Cdh1*-deleted organoids. However, Wnt5a did not affect the expansion of *Kras* or *Notch*-induced IGC organoids (data not shown).

We compared these murine DGC findings with human DGC samples. Histologically, the DGC lesions in the *Cdh1*$^{\Delta Mist1}$ mice appeared quite similar to early DGC with E-cadherin loss in patient samples (Figure 7F). Importantly, Cxcl12$^+$ cells were found in stromal cells that appeared similar histologically to blood vessels, with KLRG1$^+$ lymphocytes surrounding the signet-ring cancer cells, consistent with a role for these cells in supporting the DGC stem cell niche.

DISCUSSION

In this study, we report four major discoveries regarding gastric stem cell and cancer biology: (1) quiescent Mist1$^+$ gastric stem

(F) FACS plots of gastric Cxcr4$^+$ cells. The top left image shows gating by CD45$^+$ and *Cxcr4*-EGFP$^+$. The top middle image shows gating by Lin$^-$. The top right image shows the ILCs are identified by IL-7R$^+$CD90.2$^+$. The bottom image shows the histograms of the indicated ILC markers.
(G) Single-cell culture of Mist1$^+$ cells (red) with or without Cxcr4$^+$ cell (green) co-culture.
(H) Relative colony forming efficiency of Mist1$^+$ cells with Cxcl12 treatment and Cxcr4$^+$ cell co-culture (n = 4/group). The colony formation efficiency of the control group is set as 1.0 in (H) and (J).
(I) *Wnt5a* gene expression in Cxcr4$^{+/-}$ ILCs and non-ILC CD45$^+$ cells (n = 3/group).
(J) Relative colony forming efficiency of Mist1$^+$ cells with Wnt5a (100 ng/ml), Cxcr4$^+$ ILCs, or *Cag*-CreERT;*Wnt5a*$^{flox/flox}$ ILCs (n = 4/group).
(K) *Cxcl12*-dsRED mouse stomach with phalloidin staining (green).
(L) *Cxcr4*-EGFP;*Cxcl12*-dsRED mouse stomach.
(M) Cell positions of Cxcr4$^+$ cells and Cxcl12$^+$ cells.
(N) Immunostaining (green) of CD31 in Cxcl12$^+$ cells (red).
(O and P) GFP expression (O) and the numbers of GFP$^+$ cells (P) in *Cxcr4*-EGFP and *Tie2*-Cre;*Cxcl12*$^{flox/flox}$;*Cxcr4*-EGFP mouse corpus (n = 30/group) (means ± SEM and $^*p < 0.05$). Scale bars represent 10 μm (B–E, K, and N) and 25 μm (G, L, and O).
See also Figure S4 and Table S1.

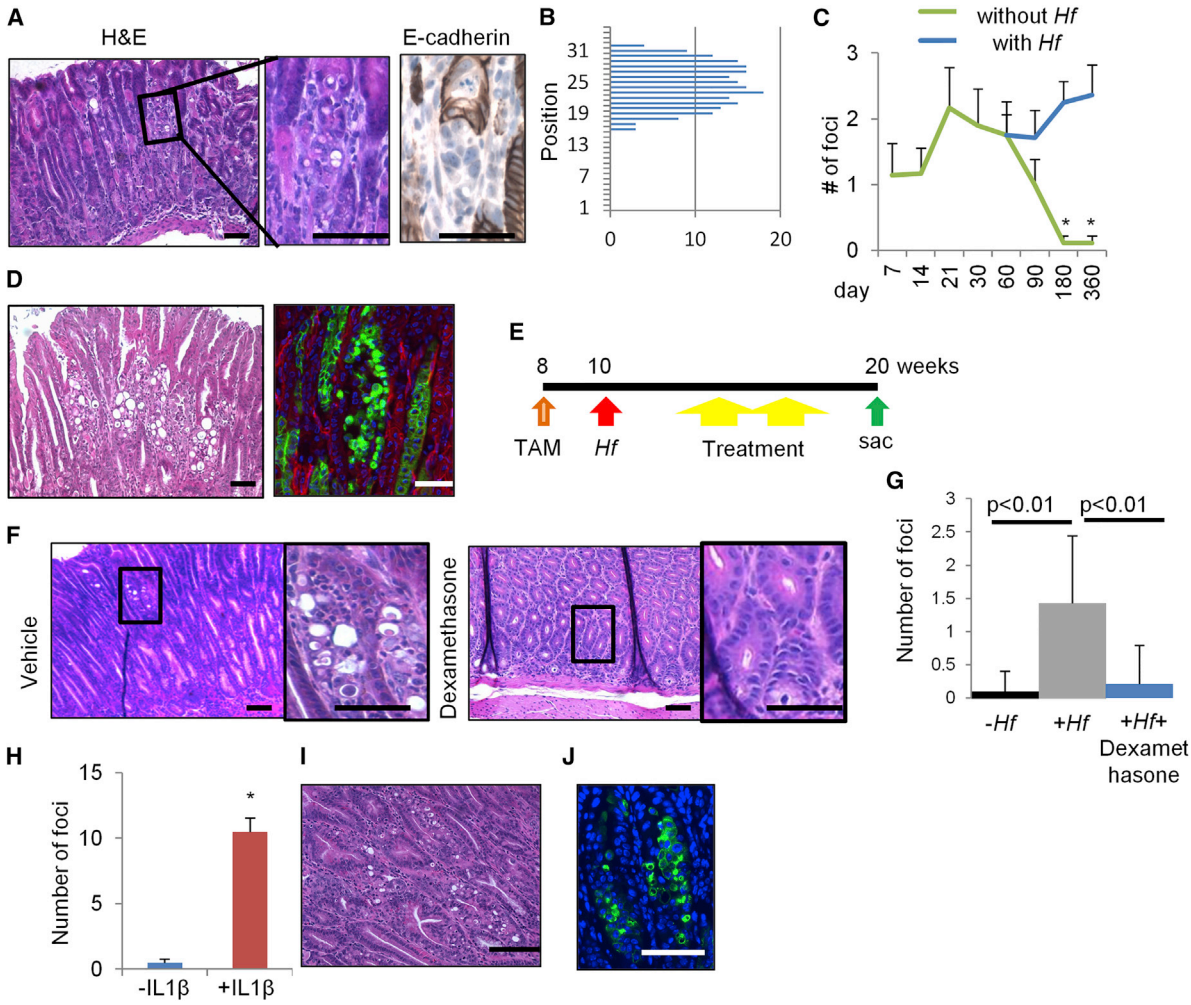

Figure 5. E-cadherin Loss in Mist1^{+} Cells Develops DGC Dependent on Chronic Inflammation

(A and B) H&E and E-cadherin staining (A) and the location (B) of atypical foci in *Cdh1*$^{\Delta Mist1}$ mice (day 10).

(C) Numbers of atypical foci per section with or without *Hf* infection (n = 3 mice/group at each time point).

(D) H&E staining (left) and GFP expression (right) in *Hf*-infected *Mist1*-CreERT2;*Cdh1*$^{flox/flox}$;*R26*-mTmG mice 18 months after TAM induction.

(E) Protocols for TAM, *Hf*, and therapies (dexamethasone, AMD3100, and anti-CD90.2 Ab).

(F and G) H&E staining (F) and numbers of atypical foci per section (G) in *Hf*-infected *Cdh1*$^{\Delta Mist1}$ mice treated with or without dexamethasone (n = 4 mice/group and four sections/mouse are analyzed).

(H–J) Numbers of atypical foci per section (H), H&E (I), and GFP staining (J) in *Cdh1*$^{\Delta Mist1}$and *Cdh1*$^{\Delta Mist1}$ mice crossed with H/K-ATPase-IL1β mice after 4 months TAM induction (means ± SEM and *p < 0.05). Scale bars represent 50 μm.

See also Figure S5.

cells located at the isthmus of the corpus gland are an origin of all epithelial lineages, (2) they can serve as a cellular origin of all histological types of gastric cancer, (3) the Cxcl12/Cxcr4 axis comprising endothelial cells and ILCs regulates the normal and neoplastic gastric stem cell niche, and (4) Wnt5a from Cxcr4^{+} ILCs promotes diffuse-type cancer growth by activating RhoA. Our data provide a focus for gastric regeneration and cancer prevention and therapy.

In the gastric corpus, the isthmus is the major site of epithelial proliferation and for many years has been thought to contain the granule free stem cell population (Karam and Leblond, 1993). We found that the isthmus Mist1^{+} cells are these granule free bona fide stem cells in the corpus, which are remarkably quiescent, dividing infrequently (every 5 days), consistent with the original expectations for mammalian adult stem cells (Malam and Cohn, 2014). It has been hypothesized that corpus glands may possess two different stem cell zones, isthmus and chief cells (Nam et al., 2010; Stange et al., 2013). Our ablation experiments using a 5-FU and *Lgr5*-DT system find that only isthmus cells, not chief cells, play a predominant role in maintaining the gastric gland and are an origin of gastric cancer. The gradient of BMP or Shh expression determines the localized expression of *Lgr5* at the gastrointestinal gland base (Shyer et al., 2015) and basal chief cells in the corpus express *Lgr5*. Thus, our model suggests that *Lgr5* expression may not always reflect actual stemness, especially in a Wnt-independent organ.

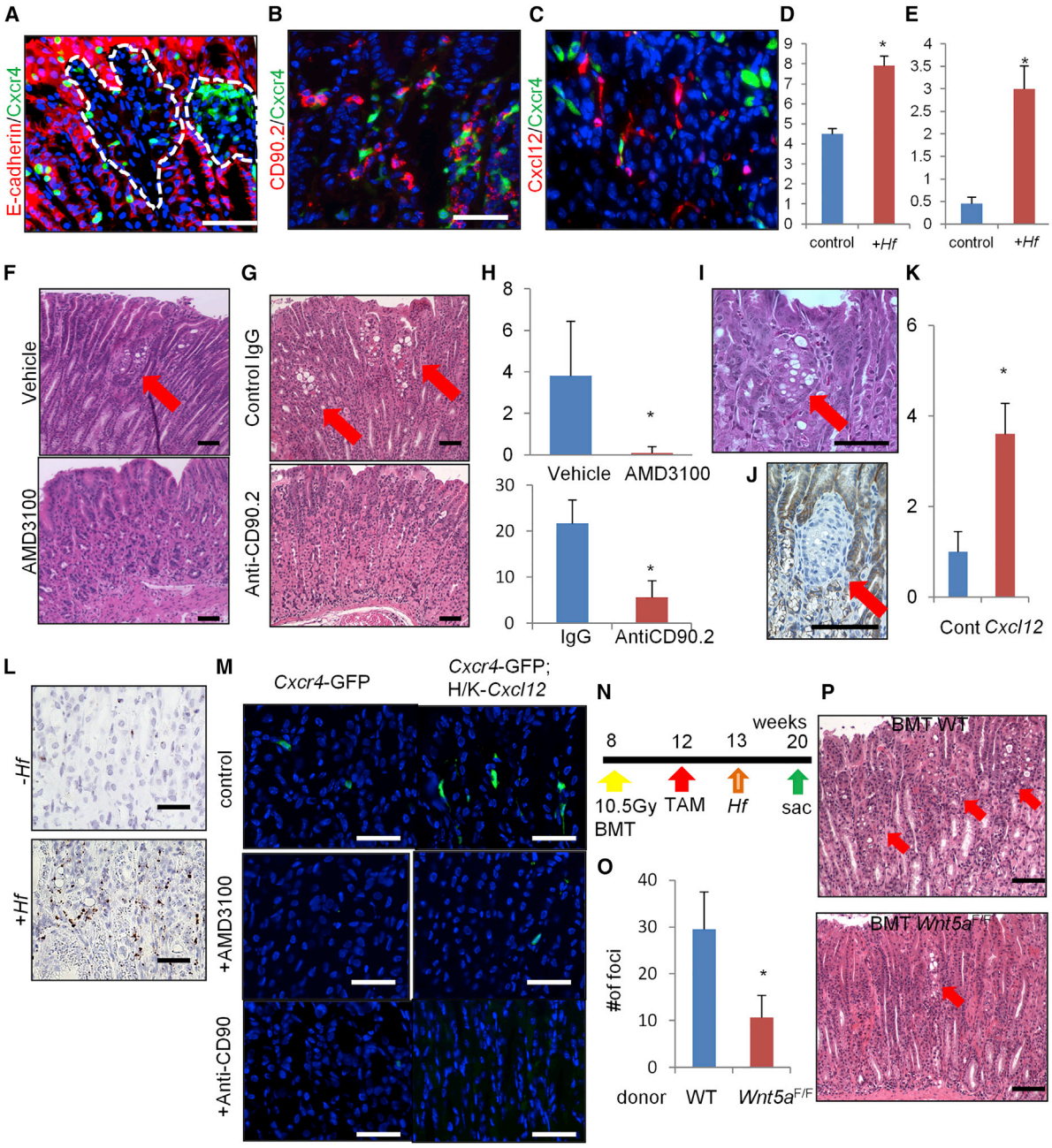

Figure 6. Cxcl12/Cxcr4 Perivascular Niche Regulates DGC Progression through Wnt5a Production

(A–E) E-cadherin (A) and CD90.2 staining (B) (red) of *Mist1*-CreERT2;*Cdh1*$^{flox/flox}$;*Cxcr4*-EGFP (green) mice, and *Mist1*-CreERT2;*Cdh1*$^{flox/flox}$;*Cxcl12*-dsRED (red);*Cxcr4*-EGFP (green) (C) mice treated with TAM and *Hf* (6 months). The numbers of Cxcl12^{+} cells (D) and Cxcr4^{+}CD90.2^{+} cells (E) per gland with or without *Hf* infection are shown. The total 20 glands per group were analyzed.

(F–H) H&E staining of *Hf*-infected *Cdh1*$^{\Delta Mist1}$ mice treated with or without AMD3100 (F) or treated with control IgG Ab or anti-CD90.2 Ab (G). The numbers of atypical foci per section (H) (n = 4 mice/group and four sections/mouse are analyzed) are shown. The arrows indicate the atypical foci.

(I–K) H&E (I) and E-cadherin (J) staining and numbers of atypical foci per section (K) in *Cdh1*$^{\Delta Mist1}$ mice crossed to H/K-ATPase-*Cxcl12* mice 3 months after TAM (n = 3 mice/group and four sections/mouse are analyzed). The arrows indicate the atypical foci.

(L) In situ hybridization of *Wnt5a* in *Cdh1*$^{\Delta Mist1}$ mice with or without *Hf* infection.

(M) *Cxcr4*-EGFP expression in WT and H/K-ATPase-*Cxcl12* mouse stomach treated with control, AMD-3100, or anti-CD90.2 Abs.

(N–P) Control or *Cag*-CreERT;*Wnt5a*$^{flox/flox}$ mouse bone marrow cells were transplanted into *Mist1*-CreERT2;H/K-ATPase-*Cxcl12*;*Cdh1*$^{flox/flox}$ mice after 10.5 Gy whole body irradiation (N). The numbers (O) of atypical foci per section and H&E staining (P) are shown (n = 4 mice/group and four sections/mouse are analyzed). The arrows indicate the atypical foci (means ± SEM and *p < 0.05). Scale bars represent 50 μm (A–C, F, G, L, and M) and 100 μm (I, J, and P).

See also Figure S6.

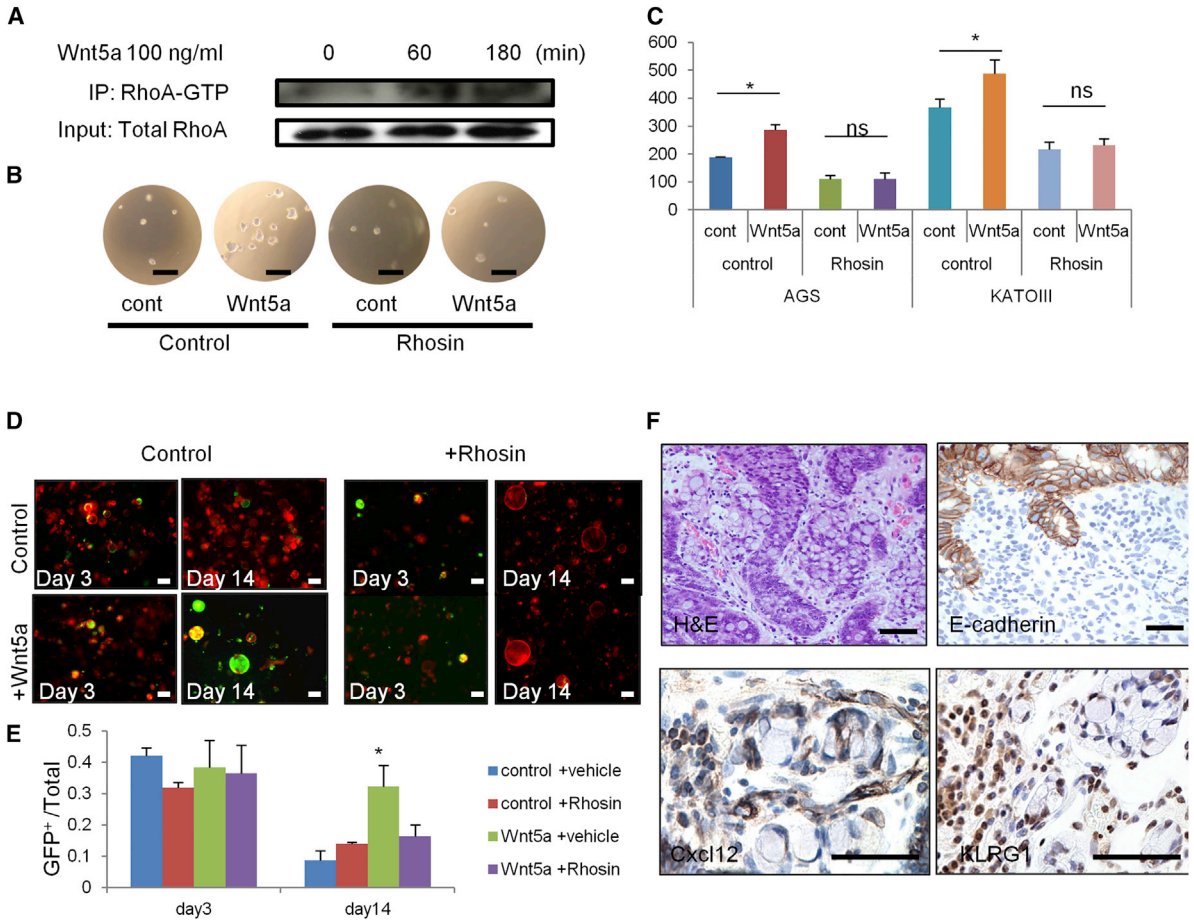

Figure 7. RhoA Activation by Wnt5a Plays a Role in DGC Development

(A) AGS cells were treated with 100 ng/ml Wnt5a for the indicated times. The cell lysates were immunoprecipitated with RhoA-GTP Ab and immunoblotted with total RhoA Ab.

(B and C) Soft-agar sphere forming assay of Wnt5a-treated AGS and KATO-III cells. The cells were treated with vehicle or 30 μM Rhosin. The sphere images (B) and numbers (C) of spheres at day 10 are shown (n = 4/group).

(D and E) Corpus organoids from TAM-treated *Mist1*-CreERT2;*Cdh1*$^{flox/flox}$;*R26*-mTmG mice treated with 100 ng/ml Wnt5a and/or 30 μM Rhosin. The images (D) and numbers (E) of GFP^{+}*Cdh1*$^{-}$ organoids per total organoid number on days 3 and 14 are shown (n = 4/group).

(F) H&E, E-cadherin, Cxcl12, and KLRG1 staining in human DGC. Scale bars represent 100 μm (D) and 50 μm (B and F) (means ± SEM and *p < 0.05).

Lineage-tracing studies have been based largely on TAM-induced Cre activation, but TAM treatment may cause epithelial cell death and influence stem cell activity (Huh et al., 2012; Zhu et al., 2013). Given that *Troy* is known to have an inhibitory effect on Wnt signaling, the knockin *Troy* lineage tracing may be related to a reduction in *Troy* expression in the knockin mice, secondary to haploinsufficiency, resulting in enhanced Wnt signaling activity in those mice. While knockin lines have many potential advantages, disruption of even one copy of the endogenous gene can apparently alter certain phenotypes.

The Cxcl12/Cxcr4 perivascular niche in the bone marrow was previously identified and studied as a major regulator of HSC (Ding and Morrison, 2013; Sugiyama et al., 2006). However, until now the role of the Cxcl12/Cxcr4 stem cell niche axis beyond the bone marrow has been unclear. In addition, Cxcl12 and Cxcr4 modulate the tumor microenvironment and targeting this axis was an effective strategy in certain cancers (Pitt et al., 2015; Quante et al., 2011; Roccaro et al., 2014). Given that human DGCs are in general extremely resistant to current treatment regimens, anti-inflammatory drugs such as steroids or non-steroidal anti-inflammatory drugs (NSAIDs), as well as specific Cxcr4 antagonists, may be useful for chemoprevention of DGC, particularly for hereditary-type DGC prior to gastrectomy, and/or for prevention of recurrent disease.

E-cadherin is essential for epithelial cell survival under normal conditions (Schneider et al., 2010) and loss of E-cadherin causes cell anoikis (Kantak and Kramer, 1998). Previous studies suggest that Cxcr4 and Wnt5a are upregulated in human gastric cancer tissues (Iwasa et al., 2009; Kanzawa et al., 2013). Recent genome-wide analyses revealed in human DGCs the presence of gain-of-function *RHOA* mutations that can inhibit anoikis (Cancer Genome Atlas Research Network, 2014; Kakiuchi et al., 2014; Wang et al., 2014). Thus, the activation of RhoA signaling, either by gene mutation or Wnt5a-mediated effect, may be essential for the development of DGC.

Wnt5a is a representative ligand that activates non-canonical Wnt signaling by binding to Ror2 to regulate cell migration, polarity, proliferation, or invasion. Wnt5a is expressed in gut stroma and contributes to intestinal elongation and colonic regeneration, however, the precise source of stromal Wnt5a has been unclear (Cervantes et al., 2009; Gregorieff et al., 2005; Miyoshi et al., 2012). We propose ILCs as a major source of Wnt5a, at least in the stomach. The function of ILCs has been highlighted in the setting of inflammatory or infectious states, although the possibility has been raised of a role for ILCs in stem cell niche or cancer development (Bando et al., 2015; Hanash et al., 2012; Kirchberger et al., 2013). Our findings would support this model, and given that ILCs are a heterogeneous population of immune cells, further efforts at detailed profiling of the ILC population in stem cell niche and cancer are needed.

EXPERIMENTAL PROCEDURES

Mice

Mist1-CreERT2 mice (Shi et al., 2009), *Cxcl12*-dsRED mice (Ding and Morrison, 2013), *Troy*$^{-/-}$ and *Troy*-BAC-CreERT2 mice (Fafilek et al., 2013), H/K-ATPase-*Cxcl12* mice (Shibata et al., 2013), *Eef1a1*-LSL-*Notch1(IC)* mice (Buonamici et al., 2009), and *Wnt5a*^{flox} mice (Miyoshi et al., 2012) were described previously. *Cxcr4*-EGFP mice were kindly provided by Richard J. Miller (Northwestern University Medical School). LSL-*Kras*^{G12D} and LSL-*Trp53*^{R172H} mice were provided by Dr. Kenneth Olive (Columbia University). *Apc*^{flox} mice were obtained from the National Cancer Institute (NCI). *Lgr5*-DTR-GFP mice were provided by Genentech. *Cdh1*^{flox}, *R26*-mTmG, *R26*-LacZ, *R26*-TdTomato, *R26*-Confetti, *R26*-EYFP, *Cxcl12*^{flox}, *Tie2*-Cre, *Id2*-GFP, and *Cag*-CreERT mice were purchased from the Jackson Laboratory. Cre recombinase was activated by oral administration of TAM (1–5 mg/0.2 ml corn oil, as indicated). All animal studies and procedures were approved by the ethics committees at Columbia University and the Academy of Sciences of the Czech Republic. Human stomach tissue sections were obtained from DGC patients who underwent surgical resection or endoscopic submucosal dissection from 2001 to 2012 at Gifu University Hospital, Gifu, Japan. All study protocols were approved by the ethics committees, and written informed consent was obtained from all patients.

Treatment

5-FU (Sigma) was administered intraperitoneally (i.p.) at a dose of 150 mg/kg. DMP-777 was given as described previously (Nam et al., 2010). DBZ was dissolved in 10% dimethyl sulfoxide and injected i.p. (30 μmol/kg) for 14 days. For Lgr5^{+} cell ablation, DT was administered i.p. at a dose of 20 mg/kg. Mice were treated with 5 mg/kg AMD3100 (Tocris) to inhibit Cxcr4 for 2 weeks, as described previously (Quante et al., 2011). Dexamethasone (Sigma) was administered i.p. at a dose of 5 mg/kg for 2 weeks. CD90.2 mAb (30H12) (BioXCell) was administered i.p. every 2 days at a dose of 250 mg/mouse for 4 weeks. Control groups were treated with appropriate vehicles or control antibodies.

SUPPLEMENTAL INFORMATION

Supplemental Information includes Supplemental Experimental Procedures, six figures, and one table and can be found with this article online at http://dx.doi.org/10.1016/j.ccell.2015.10.003.

AUTHOR CONTRIBUTIONS

Y.H. and H.A. contributed equally to the design of the experiments, performance of the animal experiments and histology, and analysis of the data. J.S., K.S., S.A., H.W., W.S., B.W.R., Y.T., X.C., W.K., S.S.K., Y. Tailor, K.N., H.T., and Z.S. performed various portions of the animal experiments. S.A. and Z.A.D. assisted with the in vitro experiments. H.T. and A.H. collected the human samples and performed the pathological evaluation. A.R.S. conducted the pathological evaluation of mice. W.S. and M.D.G. performed electron microscopy. L.D. and S.F.K. provided the mice. S.S. assisted in situ hybridization and adenovirus injection experiments. Y.H., H.A., S.A., C.B.W., L.D., J.G.F., R.A.F., D.L.W., V.K., and T.C.W. wrote the manuscript and contributed to the study supervision and coordination as well as to the performance of the experiments.

ACKNOWLEDGMENTS

We thank Dr. Anil Rustgi, Dr. Kenneth Olive, Dr. Terry Yamaguchi, Dr. Leonard H. Augenlicht, Dr. Carrie Shawber, and Dr. Richard J. Miller for providing the mice; Ms. Kristie Gordon for assisting in the fluorescence-activated cell sorting (FACS) analysis; Mr. Adam White and Ms. Theresa Swayne for producing the 3D images; Dr. Rani Sellers, Ms. Barbara Cannella, and Ms. Supreet Kainth for assisting with the in situ hybridization; Ms. Ashlesha Muley and Mr. Tao Su for technical assistance; Ms. Wendy Beth Jackelow (Medical & Scientific Illustration) for creating schematic images; and Dr. James R. Goldenring for providing DMP-777.

This research was supported by NIH grants U54CA126513, R01CA093405, R01CA120979, and R01DK052778 and by the Clyde Wu Family Foundation (T.C.W.). Y.H. was supported by Mitsukoshi Health and Welfare Foundation, JSPS Postdoctoral Fellowships for Research Abroad, and the Uehara Memorial Foundation. J.S. and V.K. were supported by the Czech Science Foundation grant numbers P305/11/1780 and 14-33952S.

Received: May 26, 2015
Revised: August 26, 2015
Accepted: October 8, 2015
Published: November 12, 2015

REFERENCES

Arnold, K., Sarkar, A., Yram, M.A., Polo, J.M., Bronson, R., Sengupta, S., Seandel, M., Geijsen, N., and Hochedlinger, K. (2011). Sox2(+) adult stem and progenitor cells are important for tissue regeneration and survival of mice. Cell Stem Cell *9*, 317–329.

Bando, J.K., Liang, H.E., and Locksley, R.M. (2015). Identification and distribution of developing innate lymphoid cells in the fetal mouse intestine. Nat. Immunol. *16*, 153–160.

Barker, N., Ridgway, R.A., van Es, J.H., van de Wetering, M., Begthel, H., van den Born, M., Danenberg, E., Clarke, A.R., Sansom, O.J., and Clevers, H. (2009). Crypt stem cells as the cells-of-origin of intestinal cancer. Nature *457*, 608–611.

Barker, N., Huch, M., Kujala, P., van de Wetering, M., Snippert, H.J., van Es, J.H., Sato, T., Stange, D.E., Begthel, H., van den Born, M., et al. (2010). Lgr5(+ve) stem cells drive self-renewal in the stomach and build long-lived gastric units in vitro. Cell Stem Cell *6*, 25–36.

Buonamici, S., Trimarchi, T., Ruocco, M.G., Reavie, L., Cathelin, S., Mar, B.G., Klinakis, A., Lukyanov, Y., Tseng, J.C., Sen, F., et al. (2009). CCR7 signalling as an essential regulator of CNS infiltration in T-cell leukaemia. Nature *459*, 1000–1004.

Cai, J., Niu, X., Chen, Y., Hu, Q., Shi, G., Wu, H., Wang, J., and Yi, J. (2008). Emodin-induced generation of reactive oxygen species inhibits RhoA activation to sensitize gastric carcinoma cells to anoikis. Neoplasia *10*, 41–51.

Cancer Genome Atlas Research Network (2014). Comprehensive molecular characterization of gastric adenocarcinoma. Nature *513*, 202–209.

Carneiro, F., Huntsman, D.G., Smyrk, T.C., Owen, D.A., Seruca, R., Pharoah, P., Caldas, C., and Sobrinho-Simões, M. (2004). Model of the early development of diffuse gastric cancer in E-cadherin mutation carriers and its implications for patient screening. J. Pathol. *203*, 681–687.

Cervantes, S., Yamaguchi, T.P., and Hebrok, M. (2009). Wnt5a is essential for intestinal elongation in mice. Dev. Biol. *326*, 285–294.

Ding, L., and Morrison, S.J. (2013). Haematopoietic stem cells and early lymphoid progenitors occupy distinct bone marrow niches. Nature *495*, 231–235.

Fafilek, B., Krausova, M., Vojtechova, M., Pospichalova, V., Tumova, L., Sloncova, E., Huranova, M., Stancikova, J., Hlavata, A., Svec, J., et al. (2013). Troy, a tumor necrosis factor receptor family member, interacts with lgr5 to inhibit wnt signaling in intestinal stem cells. Gastroenterology *144*, 381–391.

Farin, H.F., Van Es, J.H., and Clevers, H. (2012). Redundant sources of Wnt regulate intestinal stem cells and promote formation of Paneth cells. Gastroenterology *143*, 1518–1529 e1517.

Gregorieff, A., Pinto, D., Begthel, H., Destrée, O., Kielman, M., and Clevers, H. (2005). Expression pattern of Wnt signaling components in the adult intestine. Gastroenterology *129*, 626–638.

Guilford, P., Hopkins, J., Harraway, J., McLeod, M., McLeod, N., Harawira, P., Taite, H., Scoular, R., Miller, A., and Reeve, A.E. (1998). E-cadherin germline mutations in familial gastric cancer. Nature *392*, 402–405.

Hanash, A.M., Dudakov, J.A., Hua, G., O'Connor, M.H., Young, L.F., Singer, N.V., West, M.L., Jenq, R.R., Holland, A.M., Kappel, L.W., et al. (2012). Interleukin-22 protects intestinal stem cells from immune-mediated tissue damage and regulates sensitivity to graft versus host disease. Immunity *37*, 339–350.

Hanoun, M., Zhang, D., Mizoguchi, T., Pinho, S., Pierce, H., Kunisaki, Y., Lacombe, J., Armstrong, S.A., Dührsen, U., and Frenette, P.S. (2014). Acute myelogenous leukemia-induced sympathetic neuropathy promotes malignancy in an altered hematopoietic stem cell niche. Cell Stem Cell *15*, 365–375.

Hayakawa, Y., Jin, G., Wang, H., Chen, X., Westphalen, C.B., Asfaha, S., Renz, B.W., Ariyama, H., Dubeykovskaya, Z.A., Takemoto, Y., et al. (2015). CCK2R identifies and regulates gastric antral stem cell states and carcinogenesis. Gut *64*, 544–553.

Hoyler, T., Klose, C.S., Souabni, A., Turqueti-Neves, A., Pfeifer, D., Rawlins, E.L., Voehringer, D., Busslinger, M., and Diefenbach, A. (2012). The transcription factor GATA-3 controls cell fate and maintenance of type 2 innate lymphoid cells. Immunity *37*, 634–648.

Huh, W.J., Khurana, S.S., Geahlen, J.H., Kohli, K., Waller, R.A., and Mills, J.C. (2012). Tamoxifen induces rapid, reversible atrophy, and metaplasia in mouse stomach. Gastroenterology *142*, 21–24 e27.

Humar, B., Fukuzawa, R., Blair, V., Dunbier, A., More, H., Charlton, A., Yang, H.K., Kim, W.H., Reeve, A.E., Martin, I., and Guilford, P. (2007). Destabilized adhesion in the gastric proliferative zone and c-Src kinase activation mark the development of early diffuse gastric cancer. Cancer Res. *67*, 2480–2489.

Iwasa, S., Yanagawa, T., Fan, J., and Katoh, R. (2009). Expression of CXCR4 and its ligand SDF-1 in intestinal-type gastric cancer is associated with lymph node and liver metastasis. Anticancer Res. *29*, 4751–4758.

Kakiuchi, M., Nishizawa, T., Ueda, H., Gotoh, K., Tanaka, A., Hayashi, A., Yamamoto, S., Tatsuno, K., Katoh, H., Watanabe, Y., et al. (2014). Recurrent gain-of-function mutations of RHOA in diffuse-type gastric carcinoma. Nat. Genet. *46*, 583–587.

Kantak, S.S., and Kramer, R.H. (1998). E-cadherin regulates anchorage-independent growth and survival in oral squamous cell carcinoma cells. J. Biol. Chem. *273*, 16953–16961.

Kanzawa, M., Semba, S., Hara, S., Itoh, T., and Yokozaki, H. (2013). WNT5A is a key regulator of the epithelial-mesenchymal transition and cancer stem cell properties in human gastric carcinoma cells. Pathobiology *80*, 235–244.

Karam, S.M., and Leblond, C.P. (1993). Dynamics of epithelial cells in the corpus of the mouse stomach. I. Identification of proliferative cell types and pinpointing of the stem cell. Anat. Rec. *236*, 259–279.

Kim, T.H., and Shivdasani, R.A. (2011). Notch signaling in stomach epithelial stem cell homeostasis. J. Exp. Med. *208*, 677–688.

Kirchberger, S., Royston, D.J., Boulard, O., Thornton, E., Franchini, F., Szabady, R.L., Harrison, O., and Powrie, F. (2013). Innate lymphoid cells sustain colon cancer through production of interleukin-22 in a mouse model. J. Exp. Med. *210*, 917–931.

Liu, J., Zhang, Y., Xu, R., Du, J., Hu, Z., Yang, L., Chen, Y., Zhu, Y., and Gu, L. (2013). PI3K/Akt-dependent phosphorylation of GSK3β and activation of RhoA regulate Wnt5a-induced gastric cancer cell migration. Cell. Signal. *25*, 447–456.

Malam, Z., and Cohn, R.D. (2014). Stem cells on alert: priming quiescent stem cells after remote injury. Cell Stem Cell *15*, 7–8.

Mendelson, A., and Frenette, P.S. (2014). Hematopoietic stem cell niche maintenance during homeostasis and regeneration. Nat. Med. *20*, 833–846.

Mills, J.C., and Shivdasani, R.A. (2011). Gastric epithelial stem cells. Gastroenterology *140*, 412–424.

Miyoshi, H., Ajima, R., Luo, C.T., Yamaguchi, T.P., and Stappenbeck, T.S. (2012). Wnt5a potentiates TGF-β signaling to promote colonic crypt regeneration after tissue injury. Science *338*, 108–113.

Nam, K.T., Lee, H.J., Sousa, J.F., Weis, V.G., O'Neal, R.L., Finke, P.E., Romero-Gallo, J., Shi, G., Mills, J.C., Peek, R.M., Jr., et al. (2010). Mature chief cells are cryptic progenitors for metaplasia in the stomach. Gastroenterology *139*, 2028–2037.e9.

Nomura, S., Yamaguchi, H., Ogawa, M., Wang, T.C., Lee, J.R., and Goldenring, J.R. (2005). Alterations in gastric mucosal lineages induced by acute oxyntic atrophy in wild-type and gastrin-deficient mice. Am. J. Physiol. Gastrointest. Liver Physiol. *288*, G362–G375.

Okumura, T., Ericksen, R.E., Takaishi, S., Wang, S.S., Dubeykovskiy, Z., Shibata, W., Betz, K.S., Muthupalani, S., Rogers, A.B., Fox, J.G., et al. (2010). K-ras mutation targeted to gastric tissue progenitor cells results in chronic inflammation, an altered microenvironment, and progression to intraepithelial neoplasia. Cancer Res. *70*, 8435–8445.

Pitt, L.A., Tikhonova, A.N., Hu, H., Trimarchi, T., King, B., Gong, Y., Sanchez-Martin, M., Tsirigos, A., Littman, D.R., Ferrando, A.A., et al. (2015). CXCL12-producing vascular endothelial niches control acute T cell leukemia maintenance. Cancer Cell *27*, 755–768.

Quante, M., Marrache, F., Goldenring, J.R., and Wang, T.C. (2010). TFF2 mRNA transcript expression marks a gland progenitor cell of the gastric oxyntic mucosa. Gastroenterology *139*, 2018–2027.e2012.

Quante, M., Tu, S.P., Tomita, H., Gonda, T., Wang, S.S., Takashi, S., Baik, G.H., Shibata, W., Diprete, B., Betz, K.S., et al. (2011). Bone marrow-derived myofibroblasts contribute to the mesenchymal stem cell niche and promote tumor growth. Cancer Cell *19*, 257–272.

Roccaro, A.M., Sacco, A., Purschke, W.G., Moschetta, M., Buchner, K., Maasch, C., Zboralski, D., Zöllner, S., Vonhoff, S., Mishima, Y., et al. (2014). SDF-1 inhibition targets the bone marrow niche for cancer therapy. Cell Rep. *9*, 118–128.

Sato, T., van Es, J.H., Snippert, H.J., Stange, D.E., Vries, R.G., van den Born, M., Barker, N., Shroyer, N.F., van de Wetering, M., and Clevers, H. (2011). Paneth cells constitute the niche for Lgr5 stem cells in intestinal crypts. Nature *469*, 415–418.

Schneider, M.R., Dahlhoff, M., Horst, D., Hirschi, B., Trülzsch, K., Müller-Höcker, J., Vogelmann, R., Allgäuer, M., Gerhard, M., Steininger, S., et al. (2010). A key role for E-cadherin in intestinal homeostasis and Paneth cell maturation. PLoS ONE *5*, e14325.

Shi, G., Zhu, L., Sun, Y., Bettencourt, R., Damsz, B., Hruban, R.H., and Konieczny, S.F. (2009). Loss of the acinar-restricted transcription factor Mist1 accelerates Kras-induced pancreatic intraepithelial neoplasia. Gastroenterology *136*, 1368–1378.

Shibata, W., Ariyama, H., Westphalen, C.B., Worthley, D.L., Muthupalani, S., Asfaha, S., Dubeykovskaya, Z., Quante, M., Fox, J.G., and Wang, T.C. (2013). Stromal cell-derived factor-1 overexpression induces gastric dysplasia through expansion of stromal myofibroblasts and epithelial progenitors. Gut *62*, 192–200.

Shimada, S., Mimata, A., Sekine, M., Mogushi, K., Akiyama, Y., Fukamachi, H., Jonkers, J., Tanaka, H., Eishi, Y., and Yuasa, Y. (2012). Synergistic tumour suppressor activity of E-cadherin and p53 in a conditional mouse model for metastatic diffuse-type gastric cancer. Gut *61*, 344–353.

Shyer, A.E., Huycke, T.R., Lee, C., Mahadevan, L., and Tabin, C.J. (2015). Bending gradients: how the intestinal stem cell gets its home. Cell *161*, 569–580.

Stange, D.E., Koo, B.K., Huch, M., Sibbel, G., Basak, O., Lyubimova, A., Kujala, P., Bartfeld, S., Koster, J., Geahlen, J.H., et al. (2013). Differentiated

Troy+ chief cells act as reserve stem cells to generate all lineages of the stomach epithelium. Cell *155*, 357–368.

Sugiyama, T., Kohara, H., Noda, M., and Nagasawa, T. (2006). Maintenance of the hematopoietic stem cell pool by CXCL12-CXCR4 chemokine signaling in bone marrow stromal cell niches. Immunity *25*, 977–988.

Tian, H., Biehs, B., Warming, S., Leong, K.G., Rangell, L., Klein, O.D., and de Sauvage, F.J. (2011). A reserve stem cell population in small intestine renders Lgr5-positive cells dispensable. Nature *478*, 255–259.

Tu, S., Bhagat, G., Cui, G., Takaishi, S., Kurt-Jones, E.A., Rickman, B., Betz, K.S., Penz-Oesterreicher, M., Bjorkdahl, O., Fox, J.G., and Wang, T.C. (2008). Overexpression of interleukin-1beta induces gastric inflammation and cancer and mobilizes myeloid-derived suppressor cells in mice. Cancer Cell *14*, 408–419.

Wang, K., Yuen, S.T., Xu, J., Lee, S.P., Yan, H.H., Shi, S.T., Siu, H.C., Deng, S., Chu, K.M., Law, S., et al. (2014). Whole-genome sequencing and comprehensive molecular profiling identify new driver mutations in gastric cancer. Nat. Genet. *46*, 573–582.

Worthley, D.L., Churchill, M., Compton, J.T., Tailor, Y., Rao, M., Si, Y., Levin, D., Schwartz, M.G., Uygur, A., Hayakawa, Y., et al. (2015). Gremlin 1 identifies a skeletal stem cell with bone, cartilage, and reticular stromal potential. Cell *160*, 269–284.

Yang, S., Pham, L.K., Liao, C.P., Frenkel, B., Reddi, A.H., and Roy-Burman, P. (2008). A novel bone morphogenetic protein signaling in heterotypic cell interactions in prostate cancer. Cancer Res. *68*, 198–205.

Zhao, C.M., Hayakawa, Y., Kodama, Y., Muthupalani, S., Westphalen, C.B., Andersen, G.T., Flatberg, A., Johannessen, H., Friedman, R.A., Renz, B.W., et al. (2014). Denervation suppresses gastric tumorigenesis. Sci. Transl. Med. *6*, 250ra115.

Zhu, Y., Huang, Y.F., Kek, C., and Bulavin, D.V. (2013). Apoptosis differently affects lineage tracing of Lgr5 and Bmi1 intestinal stem cell populations. Cell Stem Cell *12*, 298–303.